Fluorescent Probes

DOI: 10.1002/anie.200700169

Environment-Sensitive Two-Photon Probe for Intracellular Free Magnesium Ions in Live Tissue**

*Hwan Myung Kim, Cheol Jung, Bo Ra Kim, Soon-Young Jung, Jin Hee Hong, Young-Gyu Ko, Kyoung J. Lee, and Bong Rae Cho**

Herein, we report a 2-acetyl-6-(dimethylamino)naphthalene-derived two-photon (TP) probe—AMg1—that can detect intracellular free Mg^{2+} in living cells and tissue. Mg^{2+} is one of the most abundant divalent metal ions in cells, and it plays crucial roles in many cellular processes such as proliferation and cell death as well as participating in the regulation of hundreds of enzymatic reactions.[1–3] To detect intracellular Mg^{2+}, a variety of membrane-permeable fluorescent probes have been developed with some of them being commercially available.[4–6] Most of them are used as their acetoxymethyl (AM) esters, which can readily undergo enzymatic hydrolysis to regenerate the metal-ion probe inside the cell.[7] However, confocal microscopy with one-photon (OP) fluorescent probes is limited for use near the tissue surface (< 100 μm).

To observe cellular events deep inside the tissue, it is crucial to use two-photon microscopy (TPM). TPM employing two near-infrared (NIR) photons for excitation offers a number of advantages over one-photon microscopy, including increased penetration depth (> 500 μm), lower tissue autofluorescence and self-absorption, as well as reduced photodamage and photobleaching.[8] The extra penetration that TPM affords is of particular interest in tissue imaging because surface preparation artifacts such as damaged cells extends over 70 μm into the brain slice interior.[9] However, most of the OP fluorescent probes presently used for TPM have small two-photon action cross sections ($\Phi\delta$) that limit their use in TPM. Another limitation associated with tissue imaging is a mistargeting problem, which results from membrane-bound probes.[4,10] As the probes can be accumulated in any membrane-enclosed structure within the cell and as the fluorescence quantum yield should be higher in the membrane than in the cytosol, it is practically difficult for the signals from membrane-bound probes to be separated from those of the probe–Mg^{2+} complex. Therefore, there is a need to develop efficient two-photon probes with 1) enhanced $\Phi\delta$ values for brighter TPM images and 2) larger spectral shifts in different environments for better discrimination between the cytosolic and membrane-bound probes.

To address both of these problems, we designed the first two-photon probe (AMg1) that has 2-acetyl-6-(dimethylamino)naphthalene as the two-photon chromophore and *o*-aminophenol-*N*,*N*,*O*-triacetic acid (APTRA) as the Mg^{2+}-selective binding site. We adopted the chromophore from Claurdan, a successful two-photon polarity probe for membranes,[11] and APTRA from Magnesium Green (MgG) and Mag-fura-2 probes,[4] with the expectation that AMg1 would emit strong two-photon excited fluorescence (TPEF) on forming a complex with Mg^{2+}. Moreover, if the AMg1–Mg^{2+} complex emits TPEF in a widely different wavelength range depending on the polarity of the environment, the emission resulting from the membrane-bound probes could be excluded from that of the AMg1–Mg^{2+} complex by using different detection windows.

AMg1 was prepared by reaction of **A** and a 2-methoxycarbonyl-methoxy-*N*,*N*-bis(methoxycarbonylmethyl)benzene-1,4-diamine derivative **I** (Scheme 1). To enhance the cell permeability, the carboxylic acid moieties were converted into AM esters (AMg1-AM).

The fluorescence spectra of AMg1-AM showed a gradual bathochromic shift with the solvent polarity (E_T^N)[12] in the order, 1,4-dioxane < DMF < EtOH < H_2O (Figure S1 and Table S1 in the Supporting Information). The large bathochromic shift with increasing solvent polarity indicates the utility of AMg1-AM as a polarity probe.

Figure 1 a and b show the spectral response of this probe toward Mg^{2+}. When Mg^{2+} was added to AMg1 in Tris buffer solution (10 mM, pH 7.05), there was a slight change in the absorption spectrum (Figure 1 a). In contrast, a dramatic increase in the fluorescence was observed with increasing Mg^{2+} concentrations probably as a result of the blocking of the photoinduced electron-transfer (PET) process by metal-ion complexation (Figure 1 b). The fluorescence enhancement factor was observed to be 17 in the presence of 100 mM Mg^{2+}. A nearly identical result was observed in the two-photon process (Figure S3 in the Supporting Information). In addition, Benesi–Hildebrand plots for Mg^{2+} and Ca^{2+} binding showed a good linear relationship, indicating 1:1 complex-

[*] H. M. Kim, C. Jung, B. R. Kim, Prof. Dr. B. R. Cho
Department of Chemistry and Center for Electro- and Photoresponsive Molecules
Korea University
1-Anamdong, Seoul 136-701 (Korea)
Fax: (+82) 2-3290-3544
E-mail: chobr@korea.ac.kr
S.-Y. Jung, Prof. Dr. Y.-G. Ko
Graduate School of Life Sciences and Biotechnology
Korea University (Korea)
Dr. J. H. Hong, Prof. Dr. K. J. Lee
National Creative Research Initiative Center for Neurodynamics and Department of Physics
Korea University (Korea)

[**] This work was supported by KRF-2004-201-C00067. J.H.H. and K.J.L. were supported by the Creative Research Initiatives of the Korean Ministry of Science and Technology. We thank Dr. Ji Ho Kim, Institut Pasteur Korea, for FLIM imaging.

Supporting information for this article is available on the WWW under http://www.angewandte.org or from the author.

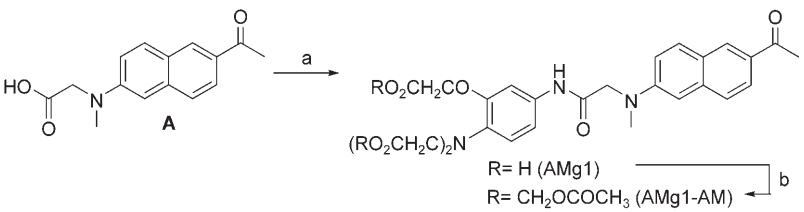

Scheme 1. Synthesis of AMg1. a) 1. **I**, EDCI, DMAP, DMF; 2. KOH, EtOH, H_2O. b) $CH_3CO_2CH_2Br$, Et_3N, $CHCl_3$. **I** = 2-Methoxycarbonyl-methoxy-*N*,*N*-bis(methoxycarbonylmethyl)benzene-1,4-diamine; EDCI = 1-ethyl-3-(3′-dimethylaminopropyl)carbodiimide; DMAP = 4-dimethylaminopyridine; DMF = *N*,*N*-dimethylformamide.

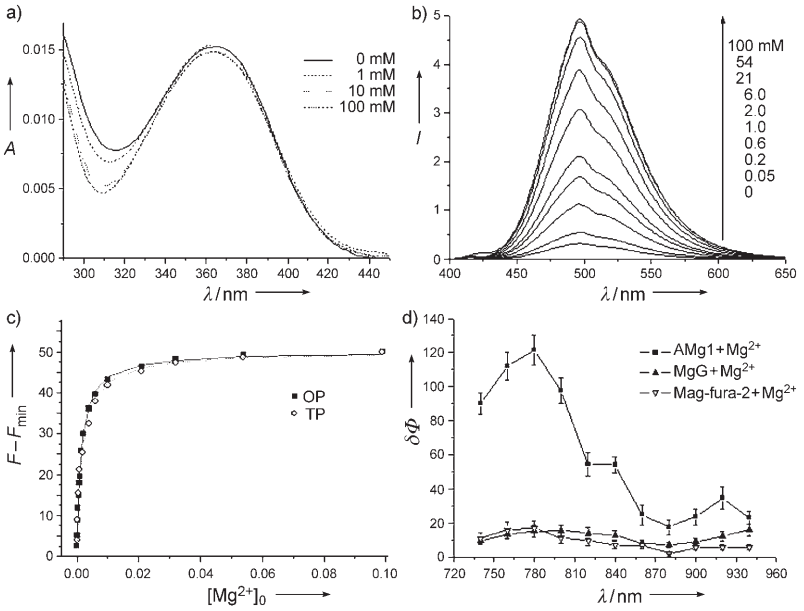

Figure 1. One-photon absorption (a) and emission (b) spectra of 1 μM AMg1 in the presence of free Mg^{2+} ions (0–100 mM). c) One- and two-photon fluorescence titration curves for the complexation of AMg1 with Mg^{2+} ions at various concentrations of free Mg^{2+} (0–100 mM). d) Two-photon action spectra of AMg1 (■), MgG (▲), and Mag-fura-2 (▽) in the presence of 50 mM free Mg^{2+}. These spectra were measured in 10 mM tris(hydroxymethyl)aminomethane (Tris), 100 mM KCl, 20 mM NaCl, 1 mM ethylene glycol-bis(2-aminoethylether)-*N*,*N*,*N*′,*N*′-tetraacetic acid (EGTA), pH 7.05. $\lambda_{ex}^{OP} = 365$ nm; $\lambda_{ex}^{TP} = 780$ nm.

ation of metal ion to probe (Figure S2 in the Supporting Information).[13]

Dissociation constants (K_d^{OP}) were calculated from the fluorescence titration curves (Figure 1c and Figure S4 in the Supporting Information).[14] The K_d^{OP} values for Mg^{2+} and Ca^{2+} were (1.4 ± 0.1) mM and (9.0 ± 0.3) μM, respectively, which were very similar to those measured for the two-photon processes [$K_d^{TP} = (1.6 \pm 0.1)$ mM (Mg^{2+}), (11 ± 1) μM (Ca^{2+})]. This result indicates the operation of a similar mechanism in both processes during the binding events.[15] The selectivity toward other metal cations is shown in Figure S5 in the Supporting Information. AMg1 showed a modest to strong response toward Mg^{2+}, Ca^{2+}, Zn^{2+}, and Mn^{2+}, and a much weaker response toward Fe^{2+}, Cu^{2+}, and Co^{2+} ions. The metal-ion selectivity of our probe is similar to those reported for MgG and Mag-Fura-2.[4] Because the intracellular concentration of free Mg^{2+} (0.1–6.0 mM) is much higher than that of Ca^{2+} (10 nM–1 μM)[4,16] and as chelatable Zn^{2+} is essentially nonexistent except in specialized areas such as the brain hippocampal CA3 region,[17] this probe can detect Mg^{2+} without interference from Ca^{2+} and Zn^{2+}. Furthermore, AMg1 and AMg1–Mg^{2+} are pH-insensitive in the biologically relevant pH range (Figure S5 in the Supporting Information).

The two-photon action spectra of the Mg^{2+} complexes of AMg1, MgG, and Mag-fura-2 in buffer solutions are depicted in Figure 1d. Table 1 shows that the $\Phi\delta$ value for the AMg1–Mg^{2+} complex is 125 GM at 780 nm, which is sevenfold larger than those for MgG–Mg^{2+} and Mag-fura-2–Mg^{2+} complexes. This result indicates that TPM images would be much brighter when stained with AMg1 than with the commercial probes.

The TPM images of AMg1-AM-labeled Hep3B cells are shown in Figure 2. Because the fluorescence quantum yields of AMg1–Mg^{2+} in Tris buffer ($\Phi = 0.58$) and AMg1-AM in DMF ($\Phi = 0.32$) are much higher than those of AMg1 ($\Phi = 0.04$) and AMg1-AM ($\Phi = 0.07$) in Tris buffer (Table 1), the TPEF emitted from the cells should be mostly due to the intracellular AMg1–Mg^{2+} complex or membrane-bound probes. Note that AMg1-AM in DMF is a good model for the latter because the λ_{max}^{fl} values are similar (Figure 2d and Figure S1b in the Supporting Information).[11] Additional evidence for this explanation was provided by the negligible TPEF emitted from the AMg1-AM-labeled Hep3B cells after treatment with 10 μM calcimycin in the presence of 2 mM ethylenediaminetetraacetic acid; the fluorescence increased upon treatment with 10 μM calcimycin in the presence of 100 mM $MgCl_2$ (Figure S7 in the Supporting Information). Moreover, the images collected at 360–620 nm showed intense spots and bright domains, with TPEF maxima at $\lambda = 440$ (blue)

Table 1: Photophysical data for magnesium ion probes.

Compound[a]	$\lambda_{max}^{(1)}$ [nm][b]	λ_{max}^{fl} [nm][b]	$\lambda_{max}^{(2)}$ [nm][c]	Φ[d]	δ_{max}[e]	$\Phi\delta$[f]
AMg1-AM	360	495	ND[g]	0.07[h]	ND[g]	ND[g]
AMg1	365	498	ND[g]	0.04	ND[g]	ND[g]
AMg1–Mg^{2+}	365	498	780	0.58	215	125
Mag-fura-2–Mg^{2+}	330[i]	491[i]	780	0.30[i]	56	17
MgG–Mg^{2+}	506[i]	532[i]	800	0.42[i]	37	16

[a] All data were measured in 10 mM Tris buffer (100 mM KCl, 20 mM NaCl, 1 mM EGTA, pH 7.05) in the absence and presence (50 mM) of $MgCl_2 \cdot 6H_2O$. [b] λ_{max} of one-photon absorption and emission spectra. [c] λ_{max} of two-photon excitation spectra. [d] Fluorescence quantum yield, ±10%. [e] The peak two-photon cross section in 10^{-50} cm^4 s/photon (GM), ±15%. [f] Two-photon action cross section. [g] Not determined. The two-photon excited fluorescence intensity was too weak to measure the cross section accurately. [h] $\Phi = 0.32 \pm 0.02$ in DMF. [i] Ref. [18].

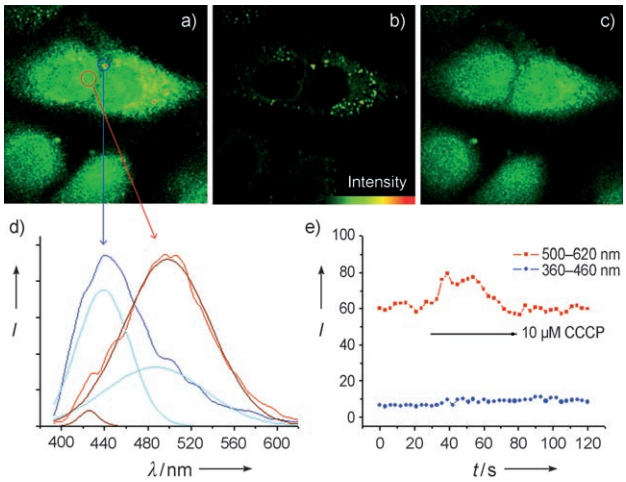

Figure 2. TPM images collected at 360–620 nm (a), 360–460 nm (b), and 500–620 nm (c) of AMg1-AM-labeled (2 μM) Hep3B cells. d) Two-photon-excited fluorescence spectra (normalized) from the hydrophobic (blue) and hydrophilic (red) domains of AMg1-AM-labeled Hep3B cells ($\lambda_{ex} = 780$ nm). The cell images shown are representative images from replicate experiments. Gaussian fits are shown in pale blue and brown. e) TPEF intensity collected at 500–620 nm (red) and 360–460 nm (blue) as a function of time.

and 498 nm (red), respectively (Figure 2a, d). Compared with the emission spectra recorded in Tris buffer, the blue band was significantly blue-shifted while the red one band nearly identical (Table 1). Both spectra could be fitted to two Gaussian functions with maxima at 439 and 488 nm (pale blue lines) and at 426 and 498 nm (brown lines), respectively (Figure 2d). It was observed that the peak positions of the dissected spectra were similar, suggesting that the probes might be located in two regions with different polarity. Furthermore, the intense spot exhibited an excited-state lifetime of 3.3 ns, which was much longer than the upper extreme of the lifetime distribution curve centered at 2.2 ns (Figure S6 in the Supporting Information). From these results, we hypothesize that the probes may be located in two different environments, a more polar one that is likely to be cytosol (red emission with a shorter lifetime) and a less polar one that is likely to be membrane-associated (blue emission with a longer lifetime).

Supporting evidence for this hypothesis was provided by study of carbonyl cyanide *m*-chlorophenylhydrazone (CCCP) activity. Because CCCP prevents the production of ATP–Mg^{2+} from ADP (ATP = adenosine triphosphate, ADP = adenosine diphosphate), inorganic phosphate, and Mg^{2+} by uncoupling oxidative phosphorylation, CCCP-treated cells should have higher levels of free Mg^{2+}.[19] When CCCP was added to the AMg1-AM-labeled Hep3B cells, the TPEF intensity in the 500–620 nm region increased immediately after addition and then decreased to the baseline level (Figure 2e). Hence, the activity of CCCP is visually confirmed by this result. In contrast, no change in the TPEF intensity was noted in the 360–460 nm range, indicating that the TPEF indeed arises from the AMg1-AM located in the cell membrane.

The errors arising from the membrane-bound probes could be minimized by detecting the TPEF from the intracellular AMg1–Mg^{2+} complex. As shown in Figure 2d, the shorter-wavelength band in the dissected Gaussian function (pale blue line) decreased to the baseline at $\lambda \approx 500$ nm. Thus, the TPEF emitted from the membrane-bound probe should be negligible at $\lambda > 500$ nm. On the other hand, if one uses AMg1-AM in DMF as a model for the latter (see above), the tail of the emission band that extends beyond 500 nm could cause an error (Figure S1b in the Supporting Information). However, the area of the tail at $\lambda > 500$ nm accounts for about 5% of the total emission band, indicating that it would not be a significant problem. Consistently, the TPEF image collected at 500–620 nm was homogeneous whereas that collected using the shorter-wavelength window of 360–460 nm clearly showed intense spots (Figure 2b, c). Therefore, one could detect Mg^{2+} ions in the 500–620 nm range with minimum contribution from the membrane-bound probes.

The intracellular Mg^{2+} concentration was determined by using $[Mg^{2+}] = K_d[(F-F_{min})/(F_{max}-F)]$ as reported (F = fluorescence intensity).[5,20] The Mg^{2+} concentration in the resting Hep3B cells was (0.65 ± 0.10) mM, in good agreement with reported values.[16] Intracellular magnesium ions have been qualitatively detected with TPM by using the newly developed probe 2,3-dicyanohydroquinone (DCHQ).[6] However, this is the first example of quantitative measurement of intracellular free Mg^{2+} ions with TPM.

To demonstrate the utility of this probe in deep-tissue imaging, acute hippocampal slices from postnatal 3-day-old mice were incubated with 5 μM AMg1-AM for 30 min at 37 °C. Figure 3a displays the brightfield image of a part of an acute mouse hippocampal slice that reveals the CA1 and CA3

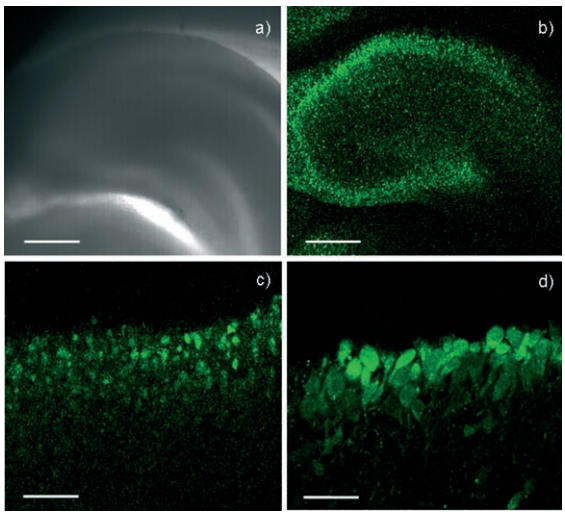

Figure 3. Images of an acute mouse hippocampal slice stained with 5 μM AMg1-AM. a) Brightfield image shows the CA1 and CA3 regions as well as the dentate gyrus upon magnification (10×). b) TPM image at the same magnification reveals the same regions at a depth of about 270 μm. c) Magnification at 40× shows the CA1 layer at a depth of around 150 μm. d) Magnification at 100× shows CA1 pyramidal neurons at a depth of approximately 150 μm. Scale bars: 300 (a, b), 120 (c), and 30 μm (d). The TPEF images were collected at 500–620 nm upon excitation at 780 nm with fs pulses.

regions as well as the dentate gyrus. The TPM image revealed Mg^{2+} distributions in the same regions at 100–300 μm depth (Figure 3b and Figure S8 in the Supporting Information), however, we cannot rule out the possibility that Zn^{2+} may have contributed in the CA3 region (see above).[17] Moreover, the images taken at higher magnifications resolved Mg^{2+} distributions in the pyramidal neuron layer of the CA1 region (Figure 3c and d), where intracellular Zn^{2+} is essentially nonexistent.[17] Furthermore, a closer examination of the image shown in Figure 3d revealed that this probe could also detect Mg^{2+} ions in the nucleus in the deep tissue. These results demonstrate that AMg1 is capable of detecting endogenous stores of labile Mg^{2+} at 100–300 μm depth in live tissues using TPM.

In conclusion, we have developed a two-photon probe for the detection of intracellular free Mg^{2+} by TPM. This probe showed 17-fold TPEF enhancement in response to Mg^{2+}, a dissociation constant (K_d^{TP}) of 1.6 mM, and sevenfold stronger TPEF than Mg-fura-2 and MgG commercial probes, and can detect intracellular free Mg^{2+} in live cells and tissue without interference from other metal ions and membrane-bound probes.

Received: January 13, 2007
Published online: April 2, 2007

Keywords: fluorescent probes · imaging agents · magnesium · two-photon processes

[1] H. Rubin, *BioEssays* **2005**, *27*, 311 – 320.
[2] R. Eskes, B. Antonsson, A. Osen-Sand, R. Montessuit, C. Richter, R. Sadoul, G. Mazzei, A. Nichols, J. C. Martinou, *J. Cell Biol.* **1998**, *143*, 217 – 224.
[3] *Magnesium and the Cell* (Ed.: N. J. Birch), Academic Press, San Diego, CA, **1993**.
[4] *A Guide to Fluorescent Probes and Labeling Technologies*, 10th ed., (Ed.: R. P. Haugland), Molecular Probes, Eugene, OR, **2005**.
[5] H. Komatsu, N. Iwasawa, D. Citterio, Y. Suzuki, T. Kubota, K. Tokuno, Y. Kitamura, K. Oka, K. Suzuki, *J. Am. Chem. Soc.* **2004**, *126*, 16353 – 16360.
[6] G. Farruggia, S. Iotti, L. Prodi, M. Montalti, N. Zaccheroni, P. B. Savage, V. Trapani, P. Sale, F. I. Wolf, *J. Am. Chem. Soc.* **2006**, *128*, 344 – 350.
[7] R. Y. Tsien, *Nature* **1981**, *290*, 527 – 528.
[8] a) W. R. Zipfel, R. M. Williams, W. W. Webb, *Nat. Biotechnol.* **2003**, *21*, 1369 – 1377; b) F. Helmchen, W. Denk, *Nat. Methods* **2005**, *2*, 932 – 940.
[9] R. M. Williams, W. R. Zipfel, W. W. Webb, *Curr. Opin. Chem. Biol.* **2001**, *5*, 603 – 608.
[10] a) C. L. Slayman, V. V. Moussatos, W. W. Webb, *J. Exp. Biol.* **1994**, *196*, 419 – 438; b) M. J. Petr, R. D. Wurster, *Cell Calcium* **1997**, *21*, 233 – 240.
[11] H. M. Kim, H.-J. Choo, S.-Y. Jung, Y.-G. Ko, W.-H. Park, S.-J. Jeon, C. H. Kim, T. Joo, B. R. Cho, *ChemBioChem* **2007**, *8*, 553 – 559.
[12] C. Reichardt, *Chem. Rev.* **1994**, *94*, 2319 – 2358.
[13] H. A. Benesi, J. H. Hildebrand, *J. Am. Chem. Soc.* **1949**, *71*, 2703 – 2707.
[14] a) J. R. Long, R. S. Drago, *J. Chem. Educ.* **1982**, *59*, 1037 – 1039; b) K. J. Hirose, *J. Inclusion Phenom. Macrocyclic Chem.* **2001**, *39*, 193 – 209.
[15] a) H. M. Kim, M.-Y. Jeong, H. C. Ahn, S.-J. Jeon, B. R. Cho, *J. Org. Chem.* **2004**, *69*, 5749 – 5751; b) H. C. Ahn, S. K. Yang, H. M. Kim, S. Li, S.-J. Jeon, B. R. Cho, *Chem. Phys. Lett.* **2005**, *410*, 312 – 315.
[16] a) J. G. Fitz, A. H. Sostman, J. P. Middleton, *Am. J. Physiol.* **1994**, *266*, G677-G684; b) M. R. Cho, H. S. Thatte, M. T. Silvia, D. E. Golan, *FASEB J.* **1999**, *13*, 677 – 683.
[17] C. C. Woodroofe, R. Masalha, K. R. Barnes, C. J. Frederickson, S. J. Lippard, *Chem. Biol.* **2004**, *11*, 1659 – 1666.
[18] H. Szmacinski, J. R. Lakowicz, *J. Fluoresc.* **1996**, *6*, 83 – 95.
[19] D. L. Nelson, M. Cox, M. Lehninger, *Principles of Biochemistry*, 4th ed., W. H. Freeman & Company, New York, **2005**, p. 707.
[20] R. E. London, *Annu. Rev. Physiol.* **1991**, *53*, 241 – 258.

